

Geoelectrical characterization of zones of disintegration in a crystalline basement environment

M. O. k'Orowe^{1,*}, V. S. Singh², V. Anand Rao² and Ratnakar Dhakate²

¹Jomo Kenyatta University of Agriculture and Technology,
P.O. Box 62000, Nairobi, Kenya

²Groundwater Exploration and Management Group,
National Geophysical Research Institute, Uppal Road,
Hyderabad 500 007, India

An attempt has been made in this study to characterize the subsurface basement structures in the Jangoan watershed in the Waipalli Basin, Nalgonda District, Andhra Pradesh, India, for identification of zones of disintegration, which are potential aquifers, using geophysical techniques. Results from resistivity inversion and tomography have been studied. A processing procedure here referred to as pseudo resistivity index parameter was initiated for characterization of basement rocks.

Keywords: Crystalline basements, electrical resistivity tomography, geoelectrical characterization, pseudo-lateral variation index.

CRYSTALLINE rocks in the study area, i.e. Jangoan watershed in the Waipalli Basin, Nalgonda District, Andhra Pradesh, India are type of hard rocks that comprise mainly of granite and granite gneiss. These rocks essentially bear no primary porosity, but with the onset of weathering, they are able to acquire secondary porosity, which has groundwater potentialities. Weathering is not a uniform phenomenon in any environment, and results in heterogeneous hydrological characteristics of the rock formations. The conceptual structure of hard rocks is that of a fresh basement overlain by materials which have undergone different stages of weathering. Groundwater availability is therefore attributed to weathering in the overburden and basement surface. Basement weathering present themselves as zones of disintegration. These zones appear as low electrical resistivity anomalies compared to the massive basement rocks that surround them. Consequently, basement troughs with deep weathering are points of disintegration, which are hydro-geologically viable as far as groundwater aquifers are concerned. A systematic scheme has therefore been initiated using Schlumberger array and electrical resistivity tomography to determine the geoelectrical characteristics of the basement rock by studying the results of inverted resistivity imaging data.

The study area is approximately 28 km² in area, and lies between long. 78.84°E and 79.92°E, lat. 17.10°N and 17.14°N. It is situated in the Narayanpur division of Nal-

gonda District (Figure 1). Low rainfall coupled with yearly decline has resulted in semi-arid conditions in the area. According to the Central Ground Water Board¹, the area is underlain by pink and grey granites, magnetite gneiss and related rocks. Rainfall is mainly from the southwest monsoon during June–September each year. Figure 2 shows the annual rainfall trends for the last seven years (1997–2004).

The lineaments were used to guide a DC resistivity-sounding programme, with 17 sounding stations located near the lineaments, wherever possible. The intention here was to map low resistivity zones that normally correspond to saturated zones. Frohlich *et al.*² conducted resistivity studies in Northern Maine on metamorphic petites and limestone, which indicated low resistivities over high-yielding fractured rocks. Schlumberger configuration was carried out in 17 spots (Figure 3). In Figure 3, *A* and *B* are current electrodes, while electrodes *M* and *N* are potential electrodes.

Figure 4 shows the lineaments and Ves-points. The electrode spacings were up to 100 m half the current electrode spacing and occasionally 120–140 m, this being determined by the rising part of the apparent resistivity curve. Soundings were terminated as and when the rising part of the curve approached a 45° inclination, which indicates resistive basement. Typical resistivity curves are shown in Figure 5.

In situations where we have a hard rock environment, basement and regolith have a marked resistivity contrast. A low value for basement may be due to some saturating component on the basal features of the basement. The resistivity values for the basement show values ranging from as low as 368.03 Ohm-m at Ves station M-15 to as high as 36,824.02 Ohm-m at station M-13. As a first approximation, station M-15 that shows a low resistivity value would be associated with at least some groundwater saturation. However, to characterize the whole basement area, krigging³ was done using SURFER software to obtain a basement resistivity contour map (Figure 6). The values for the basement resistivities were high towards the north and northeast of the area. This could be as a result of the basement being closer to the surface. Since the topography to the north and northeast indicates presence of a hillock, basement topography should follow the surface relief. To the south of the area where contour lines are less than the 5000 Ohm-m, relatively smooth and widely spaced contours were seen. This would suggest a uniform bedrock resistivity with absence of any lateral variation features like fractures or zones of disintegration. The high basement resistivities noticed for this area however make the contours visually insensitive to lateral variations. A processing method to enhance the resistivity variation was therefore developed. The lateral variation index used by Olayinka and Barker⁴, which measures resistivity variation along a 2D profile has been modified. The index thus modified is referred here as a pseudo-lateral variation

*For correspondence. (e-mail: modondi@yahoo.com)

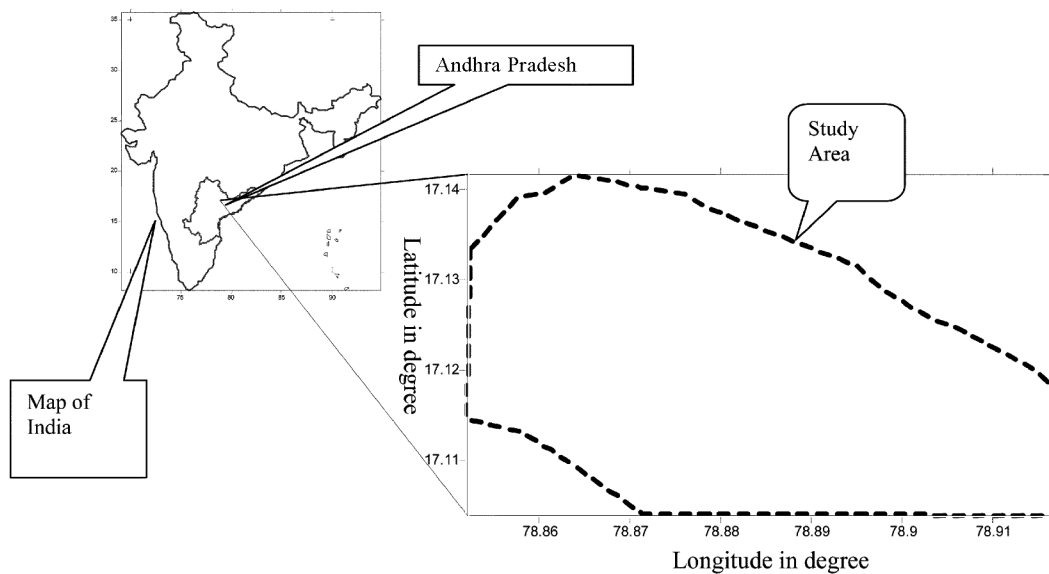


Figure 1. Map of India showing the study area.

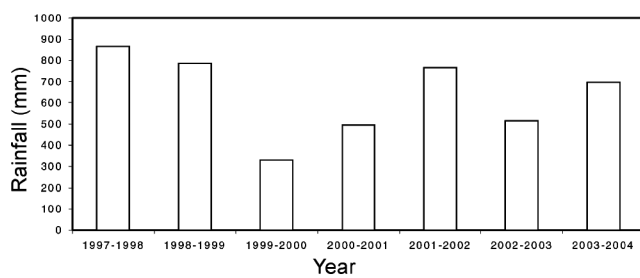


Figure 2. Mean annual rainfall.

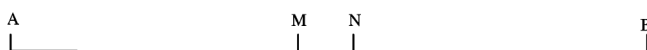


Figure 3. Schlumberger array configuration.

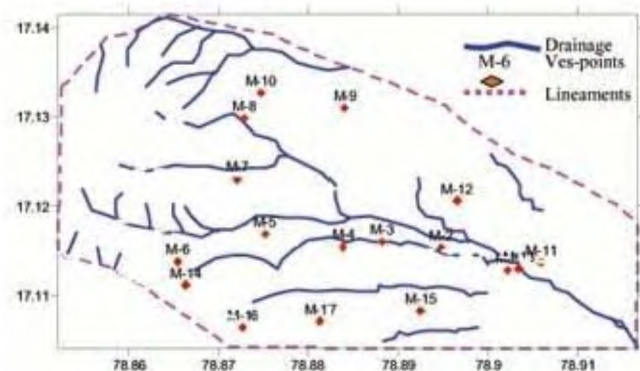


Figure 4. Map showing Ves-points, lineaments and drainage.

index. In this format it is not uni-directional, but measures a lateral variation in all directions around a particular point in relation to its neighbouring points. The expression is of the form:

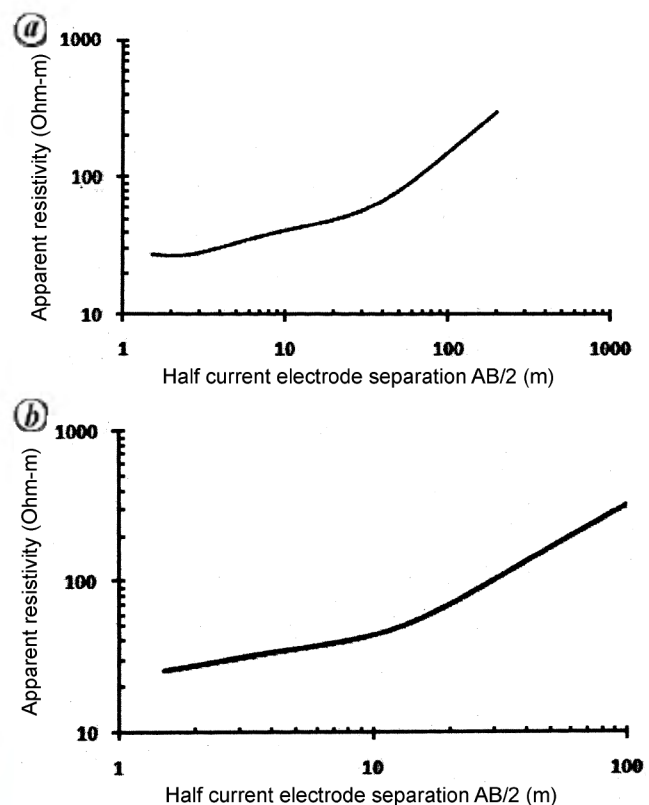


Figure 5. Resistivity curve for (a) M-6 and (b) M-7.

$$PLVI\left(n + \frac{h}{2}\right) = \left| \frac{\rho_{(n+h)} - \rho_n}{\frac{1}{2}[\rho_{(n+h)} + \rho_n]} \right| \times 100\%,$$

where PLVI is the pseudo lateral variation index at a point midway between any point n and another one located

at a distance h away. ρ_n and ρ_{n+h} are the values of apparent resistivities at points n and $n+h$ respectively. A study of the PLVI contours (Figure 7) indicates high variation index anomalies at points between Ves-stations M-3 and M-2. The closely spaced steep contours are probably due to rapid resistivity changes in the bedrock at those locations. The anomalies should mark lateral geoelectrical boundaries, which were not so apparent on the contour map of basement resistivity.

From the PLVI contours, the anomalous zone M-3, moderately anomalous zone M-17 and a flat zone M-15 were chosen for deep sounding using stacking metres up to spreads ($AB/2$) between 180 and 220 m. The current electrode spacing was increased at intervals of 5 m after the spread had attained values beyond 20 m, while $MN/2$ was kept constant at 2 m. This was done so that any small variation in the apparent resistivity values could be detected.

Among the three locations where long-spread sounding was done, only the curve obtained at M-3 (Figure 8a) showed an inflection at greater spacing, indicating an anomaly at depth. The other points M-15 (Figure 8b) and M-17 (Figure 8c) showed no inflection of resistivity trend at large separation. Electrical resistivity tomography was then conducted at point M-3, to verify the course of

inflection. Though the relationship between spacing and apparent resistivity is a power function, we have used a linear representation in Figure 6 because the incremental spacing between the current spacing is short (increments of 5 m), so that resistivity transitions are expected to be gradual. Any sudden change is indicative of an anomalous resistivity zone in the basement, as a result of either a fracture or density variation, both factors associated with groundwater saturation.

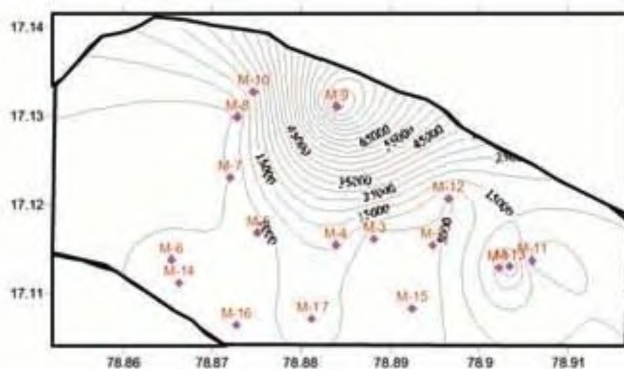


Figure 6. Basement resistivity distribution.

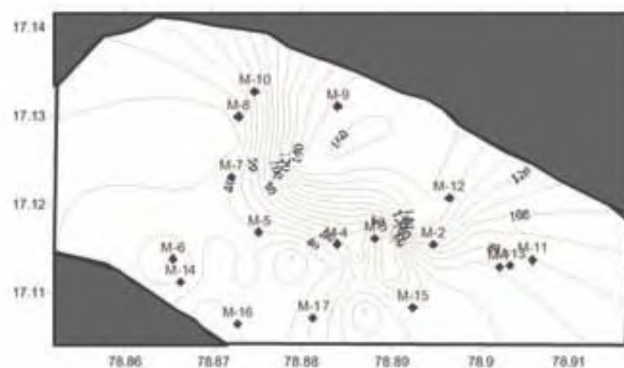


Figure 7. Pseudo-lateral variation index distribution.

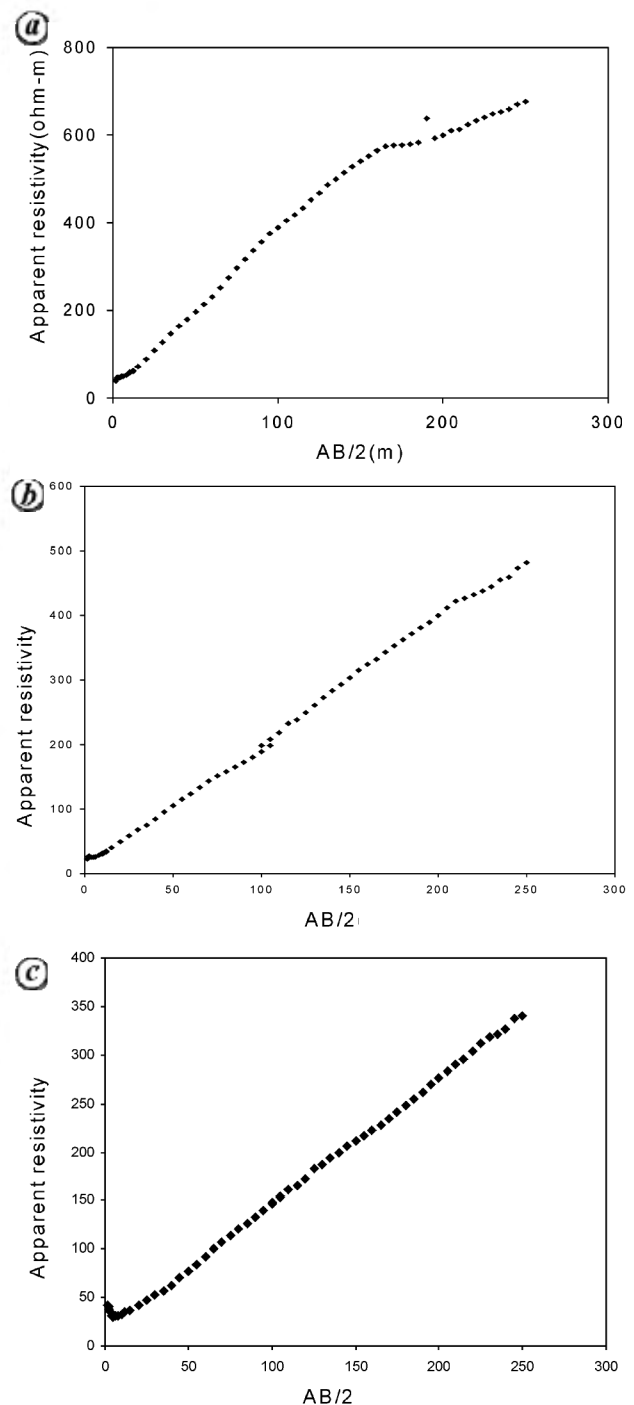


Figure 8. Long-spread sounding locations: a, M-3; b, M-15; c, M-17.

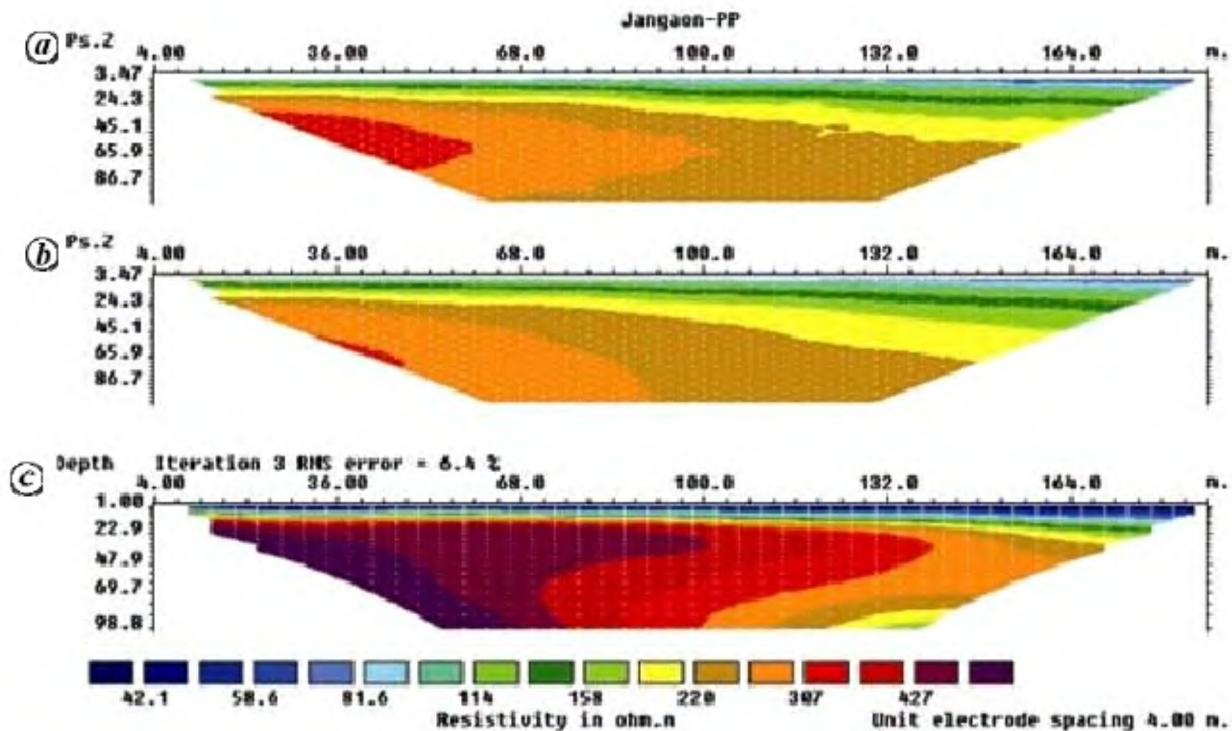


Figure 9. *a*, Measured apparent resistivity pseudosection; *b*, Calculated pseudosection, and *c*, Inverse model.

A 2-D resistivity survey characterizes both the lateral as well as vertical variations along a profile. A SYSCAL Jr Switch 48 (IRISH Inst.) resistivity meter was utilized in this study. The electrodes (48 nos), which are about 0.3 m in length and made of stainless steel, were watered to improve ground contact and then laid out along the line at intervals of 4 m. They were then connected to a system that automatically switches between appropriate configurations. At any time, four electrodes were automatically chosen for measurement. One image line was measured at point M-3. The base or the first electrode position faced the eastern end of the profile; the last position was towards the hillocks to the west. The line length was 200 m. This method has been used successfully before for imaging subsurface resistivities of environmental, hydrological as well as engineering targets^{5,6}. Two types of linear arrays were used in this study, namely pole–pole and Schlumberger/Wenner⁵ configurations. In the pole–pole configuration, the current electrode *A* and the potential electrode *M* were kept at infinity (500 m in our case). The orientation was perpendicular to the east–west profile of our tomography line.

The data were processed⁶ using the inversion software RES2DINV version 3.42, which produced inverted resistivity sections from apparent resistivity measurements. The method entails a least squares scheme, which is used to fit calculated resistivities, to model the subsurface structure. The tomography that was eventually reconstructed is presented as apparent resistivity model cross-sections.

The images are presented for the pole–pole configuration in Figure 9. Figure 9*a* shows the observed apparent resistivity data plotted as a pseudo-section against $AB/2$, while Figure 9*b* shows the computed sections. The two models have a clear similarity, which attests to the accuracy of the inversion. Figure 9*c* shows the true resistivity and true depths of the subsurface structures generated by inversion of the input data.

In this study the result obtained from the pole–pole configuration shows a low resistivity layer, which signifies a weathered horizon at shallow depths between 2 and 12 m, with resistivities ranging from 68 to 190 Ohm-m, according to the colour code. The topsoil has resistivity in the range 22–68 Ohm-m; at depths less than 2 m this is representative of soil rich in clay. The bedrock here has resistivity of more than 300 Ohm-m. A low resistivity horizon is indicated below the electrode number 96, which is the centre of the survey line, as can be seen from the dip downward towards low resistivity values. This is seen to occur at depths greater than 90 m. Fractures are unfortunately not indicated directly in this image. However, a low resistivity layer is seen at depth below electrode number 96, which is at the centre of the line profile. This shows that weathering has occurred, which could result into bedrock fracture at depth.

The imaging technique correlated well with the long spread sounding in determining low resistivity zones within the basement rocks. The PLVI index has also been shown to be a good indicator of geoelectric boundaries in the

highly resistive basement rocks. The techniques applied here were however insufficient to locate lineaments, which were indicated in the area from satellite imageries.

1. Central Groundwater Board, Ministry of Water Resources, Government of India, Occurrence, genesis and control strategies of fluoride Waipalli watershed, Nalgonda District, Andhra Pradesh, India, 2003.
2. Frohlich, R. K., Williams, J. B. and Boland, M. P., A geological study of hydraulic bedrock conditions in Aroostook County, Maine. In Proc. Symp. of Int. Conf. on Fluid Flow in Fractured Rocks, Atlanta, May 1988, pp. 114–124.
3. De Marsily, G., Spatial variability and uncertainty in porous media; a stochastic approach. In *Fundamentals of Transport Phenomena in Porous Media* (ed. Bear, J.), The Hague, 1986.
4. Olayinka, A. I. and Barker, R. D., Borehole sitting in crystalline basement areas of Nigeria, with micro-processor controlled resistivity-traversing system. *Groundwater*, 1990, **28**, 178–183.
5. Loke, M. H. and Barker, R. D., Rapid least squares inversion of apparent resistivity pseudo-sections by a quasi-Newton method. *Geophys. Prospect.*, 1996, **44**, 131–152.
6. Loke, M. H., Electrical imaging surveys for environmental and engineering studies – A practical guide to 2D and 3D surveys, 2000; info@terraplus.com

ACKNOWLEDGEMENTS. We are grateful to the Director, National Geophysical Research Institute (NGRI), Hyderabad for permission to publish this work. We also thank financial assistance provided by the Council of Scientific and Industrial Research, New Delhi and the Third World Academy of Sciences for providing financial assistance through the award of a postgraduate fellowship to the M.O.k.O. at NGRI.

Received 3 January 2007; revised accepted 8 September 2008

Liquefaction features of the 2005 Muzaffarabad–Kashmir earthquake and evidence of palaeoearthquakes near Jammu, Kashmir Himalaya

R. Jayangondaperumal^{1,2}, V. C. Thakur^{1,*} and N. Suresh¹

¹Wadia Institute of Himalayan Geology, Dehradun 248 001, India

²Present address: Centre for Geotechnology, M.S. University, Tirunelveli 627 012, India

We have studied the earthquake-induced ground deformation features like fractures and landslides associated with the 2005 Muzaffarabad–Kashmir earthquake. During the study we observed well-developed liquefaction features at Simbal camp, about 20 km south of Jammu. We excavated small trenches for palaeoseis-

mological study at the site. We recorded two palaeo-earthquake events (I and II) of sand injections prior to the sand blows of the 2005 earthquake. Two palaeo-earthquakes events have been interpreted in the trench. Event-II is assigned an age of 2000 yrs BP (i.e. beginning of the first millennium) and the event-I occurred during AD ~1100. The Main Boundary Fault, locally called the Riasi thrust, lies along the southeastern extension of the Balakot–Bagh Fault. The liquefaction features are located around ~240 km SE of the epicentre of the 2005 event, and may have been produced due to favourable ground conditions and dynamic stress transfer, as the rupture and stress are reported to have propagated to the SE from the epicentral area.

Keywords: Fractures, landslides, liquefaction features, palaeoseismology, sand blows.

THE 8 October 2005 Muzaffarabad–Kashmir earthquake ($M_w = 7.6$) was the deadliest in the history of the Indian subcontinent that killed more than 80,000 people. The earthquake occurred on a rupture plane 75 km long and 35 km wide^{1,2} with strike of 331° and dip angle of 29° . The epicentre of the event was located north of Muzaffarabad (34.493°N and 73.629°E) within the Hazara Syntax and about 120 km WNW of Srinagar (USGS, NEIC WDCS-D; Figure 1). A surface rupture called the Balakot–Bagh Fault (BBF), 75 km long with variable slip of 3–5.5 m has been recorded and mapped in the field for an Himalayan earthquake^{3–5}. Based on surface displacements deduced from GPS observations and locations of aftershocks, it has been suggested that the earthquake may have originated from multiple fault planes⁶. The post-earthquake field observations and general hazard assessment associated with the October event in the eastern part of the line of control (LOC) has been reported recently⁷.

During a field survey undertaken two weeks after the earthquake, we mapped the surface ground fractures in the Tangdhar–Titwal, Uri and Punch–Rajouri sectors and liquefaction features in Jammu areas. The orientations and displacements recorded in the fractures reflect pronounced strike-slip together with some tensile component⁸. The Tangdhar–Titwal area, lying on the hanging wall of the causative fault show left-lateral strike-slip motion, and the Uri region showing right-lateral strike-slip movement is located towards the southeastern extension of the causative fault zone (Figure 1). The shear fractures are related to static stress that was responsible for the failure of the causative fault. In Jammu area, located ~240 km southeast of the epicentre, the fractures and the liquefaction features were produced as a result of favourable ground conditions and may be due to propagation of dynamic seismic waves⁸.

Jammu city is located within the outermost part of the Sub-Himalaya in the Siwalik range made of conglomerate and sandstone of upper Siwalik. South of the range front,

*For correspondence. (e-mail: thakurvc@wihg.res.in)